Effects of interstitial additions on the structure of Ti_5Si_3

J.J. Williams, M.J. Kramer, and M. Akinc
Ames Laboratory and Department of Materials Science and Engineering, Iowa State University, Ames, Iowa 50011

S.K. Malik
Tata Institute of Fundamental Research, Bombay 400005, India, and University of Missouri Research Reactor, Columbia, Missouri 65211

(Received 3 August 1999; accepted 24 May 2000)

Changes in the structure of Ti_5Si_3 were measured by x-ray and neutron diffraction as carbon, nitrogen, or oxygen atoms were systematically incorporated into the lattice. Additionally, the lattice parameters and variable atomic positions of pure Ti_5Si_3 were determined to be $a = 7.460$ Å, $c = 5.152$ Å, $x_{Ti} = 0.2509$, and $x_{Si} = 0.6072$. The measured trends in lattice parameters as carbon, nitrogen, or oxygen atoms were added to Ti_5Si_3 showed that most of the previous studies on supposedly pure Ti_5Si_3 were actually contaminated by these pervasive light elements. Also, oxygen and carbon additions were shown to strongly draw in the surrounding titanium atoms—evidence for bonding between these atoms. The bonding changes that occurred on addition of carbon, nitrogen, or oxygen acted to decrease the measured anisotropic properties of Ti_5Si_3, such as thermal expansion.

I. INTRODUCTION

Published values of the lattice, thermodynamic quantities, and thermal properties of Ti_5Si_3 from 1985 to present show considerable scatter. For example, published lattice parameters vary by 0.5%,[1–6] thermal expansion coefficients by 90%,[4–8] and enthalpy of formation by 15%,[2,9,10] all of which are significant variations. Without question, a primary reason for this scatter in properties is the presence of interstitial impurities. Two recent studies by Radhakrishnan *et al.*[11] and Thom and Akinc[12] highlight the improbability of synthesizing and consolidating Ti_5Si_3 without interstitial contamination of carbon, nitrogen, and oxygen. Particularly, studies that use metal powder as a starting material are highly likely to result in oxygen impurity of at least one to two weight percent. Not only titanium powder, but yttrium, zirconium, and other early transition metal powders that have a high affinity for carbon, nitrogen, and oxygen are expected to yield silicides with a significant impurity content after synthesis and processing. Furthermore, studies on Ti_5Si_3 with carbon, nitrogen, or oxygen intentionally added show a very dramatic effect on crystal and thermal properties, an effect that does account for some of the scatter in the literature data. For example, Thom *et al.*[5] have shown a reduction in thermal expansion anisotropy by 20% when carbon is intentionally added to Ti_5Si_3.

In conjunction with contaminated starting materials, an additional reason for the difficulty in synthesizing Ti_5Si_3 without impurities is the presence of large, unoccupied interstices in the lattice. Figure 1(a) shows a (001) orthographic projection of the hexagonal Ti_5Si_3 lattice, which has Mn_5Si_3 as its prototype structure (space group = $P6_3/mcm$). The occupied atomic sites for pure Ti_5Si_3 are Ti at 4d sites at (⅓, ⅔, 0), Ti at 6*g* sites at (x_{Ti}, 0, ¼), where $x_{Ti} \approx 0.25$, and Si at 6*g* sites at (x_{Si}, 0, ¼), where $x_{Si} \approx 0.61$. Impurity atoms of carbon, nitrogen, and oxygen would occupy interstices located at (0, 0, 0) 2*b* sites, herein described as Z sites. As seen in Fig. 1(b), these interstices and the surrounding Ti^{6g} atoms form trigonal antiprisms along the *c* axis. This may be alternatively described as a chain of (trigonally distorted) face-shared octahedra formed by Ti^{6g} atoms along the *c* axis with a Z site at the center of each octahedron. The Si atoms form a chain of distorted face-shared trigonal antiprisms also parallel to the *c* axis such that one Ti^{4d} site is at the center of each antiprism. This leads to a stacking sequence along the *c* axis of ABAC where A planes consist solely of Z and Ti^{4d} sites. The B and C planes contain the Ti^{6g} and Si sites such that atoms on B planes are rotated 180° with respect to atoms on C planes.

The primary goal of this study is to measure changes in lattice parameters and atomic positions by x-ray and neutron diffraction when carbon, nitrogen, or oxygen is intentionally added to Ti_5Si_3. Because purity is of utmost concern, samples were synthesized via arc melting of bulk pieces, not powders. Knowledge of lattice changes as a function of interstitial content can be used to estimate the compositions of previous studies that reported

the lattice parameters of supposedly pure Ti_5Si_3. This will aid in deconvoluting the inherent properties of Ti_5Si_3 from those of Ti_5Si_3 contaminated with carbon, nitrogen, and oxygen. Additionally, changes in bonding may be inferred from the measured structural changes on addition of interstitial atoms to aid in explaining the effects of interstitial content on the thermal and electronic properties of Ti_5Si_3.

Three systematic studies currently exist on the effects of interstitial content on the structure of Ti_5Si_3. One by Kajitani *et al.*[1] has shown that interstitial hydrogen tends to contract the *a* axis and expand the *c* axis. Another study, by Thom and Akinc,[12] has shown that interstitial nitrogen and oxygen tend to contract both the *a* axis and *c* axis. The measured trend in lattice as a function of nitrogen enabled Thom and Akinc[12] to estimate the level of nitrogen impurity in a sample synthesized by Quakernaat and Visser[13] based on Quakernaat's reported lattice parameters. The third study by Thom *et al.*[14] measured the lattice changes by single-crystal and powder x-ray diffraction of $Ti_5Si_3Z_X$ for Z = boron, carbon, nitrogen, or oxygen. Whereas the effects of nitrogen and oxygen were identical to the previous study, boron and carbon tended to expand the lattice, probably because of their larger size. All interstitial additions tended to pull in the surrounding titanium atoms, which indicates a significant change in bonding. This bonding change could aid in explaining an interstitial atom's effect on the thermal and electric properties.

Unlike previous studies, this study includes structural refinements at several levels of interstitial content for each interstitial atom so that trends may be clearly discerned. Also, a strong effort was made to improve the sampling statistics and measurement accuracy over those of previous studies.

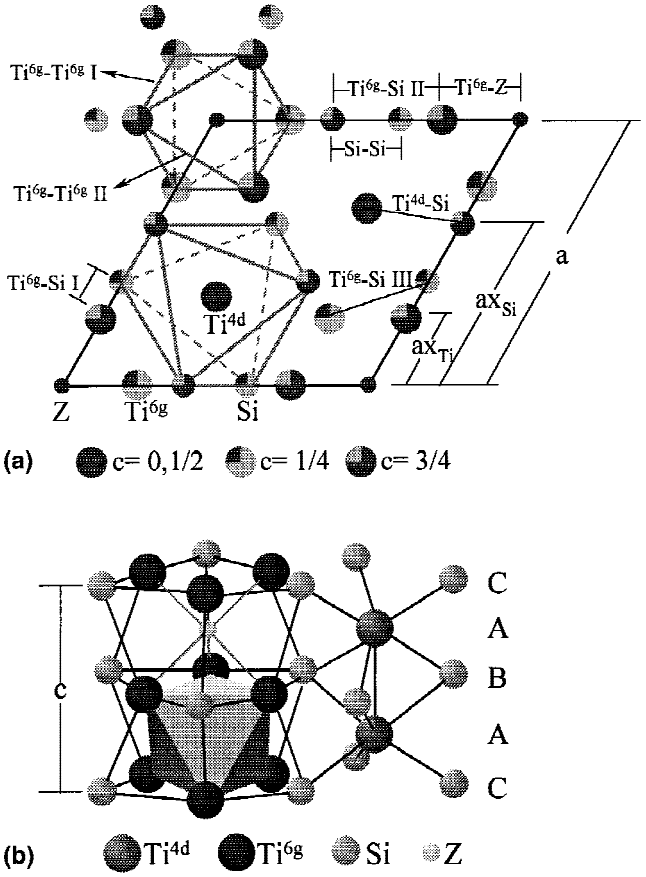

FIG. 1. (a) (001) Orthographic projection of the Ti_5Si_3Z crystal structure. The Ti^{6g} octahedra and Si antiprisms are outlined at top left and bottom left, respectively. Both the Ti^{6g} and Si atoms occupy variable positions along the <100> direction, x_{Ti} and x_{Si}. (b) Portion of the $Ti_5Si_3Z_X$ crystal structure, illustrating how the antiprisms, which are higlighted in (a), are stacked along the *c* axis. Also note the ABAC stacking sequence along the *c* axis.

II. EXPERIMENTAL PROCEDURE

All materials in this study were synthesized via arc melting. Arc melting was performed in an ultrahigh-purity argon atmosphere on a water-chilled copper hearth. Samples, which weighed approximately 10 g each, were melted at least three times via a nonconsumable tungsten electrode. This procedure led to weight losses of less than 0.5 wt% in most samples. The likely reasons for weight loss were due to use of starting materials with high rates of disassociation (TiO_2 and TiN) at arc-melting temperatures and spalling of brittle materials (Ti_5Si_3, Si, TiO_2, and TiN) during arc melting.

The starting materials included sponge titanium (Timet, Henderson, NV, 99.7 wt%), silicon pieces (Alfa Æsar, Ward Hill, MA, 99.9999 wt%), spectrographic-grade graphite electrodes for carbon, titanium nitride for nitrogen (Johnson Matthey, Ward Hill, MA, 99.8 wt%), and titanium dioxide for oxygen (Fisher Scientific, Pittsburgh, PA, 99.8 wt%). The sponge titanium was premelted two times to volatilize surface contamination before being used in synthesis of $Ti_5Si_3Z_X$. Also, the titanium nitride and oxide, which were purchased as powders, were pressed into pellets and partially sintered before using. This practice reduces material loss because the force exerted by an electric arc easily blows around powders. X-ray diffraction (XRD) and metallography on the starting materials have confirmed that they were single phase. Additionally, lattice parameter measurements for TiN and TiO_2 have shown them to be on stoichiometry, and lattice parameters for the titanium metal indicate a negligible interstitial content.

Changes in lattice parameters of Ti_5Si_3 on addition of carbon, nitrogen, or oxygen were measured by XRD (Model X1 with solid-state detector, Scintag, Sunnydale, CA). Samples were of arc-melted material ground to <20 μm in an agate mortar with 10 wt% silicon (SRM 640b, National Institute of Standards and Technology, Gaithersburg, MD) added as an internal standard. Dif-

fraction scans were run on 0.15 g samples from a 2θ of 10° to 130° at a step size of 0.03° and counting time of 3 s. The x-ray source was copper K_α; the source and detector slits were 2 to 4 mm and 0.5 to 0.3 mm, respectively. Lattice parameters, atomic positions, thermal parameters, and preferred orientations were refined using Rietveld software (GSAS, Los Alamos National Laboratory, Los Alamos, NM, 1985). Generally, the standard error of measurement was less than 0.0001 Å for lattice parameters and less than 0.001 Å for atomic positions. The weighted residuals, wR_p, were 0.10 to 0.15 for samples with interstitial carbon or oxygen and 0.15 to 0.20 for samples with interstitial nitrogen. The weighted residual function is defined as a sum over the entire diffraction pattern:

$$wR_p = [\Sigma\ w(I_o - I_c)^2]/[\Sigma\ wI_o^2] \quad , \qquad (1)$$

where I_o is the observed intensity, I_c the calculated intensity, and the weights, w, are assumed to be uncorrelated. On average, $Ti_5Si_3N_X$ compositions yielded measurably broader diffraction lines than other samples. Specifically, samples with nitrogen were on average 20% broader than the silicon standard (lines from samples with carbon and oxygen were similar in width to those of the silicon standard). This broadening suggests a slight heterogeneity and/or a higher defect concentration.

Using the Missouri University Research Reactor (MURR), the atomic positions and site occupancies of $Ti_5Si_3C_X$, (X = 0.15, 0.25, and 0.5; nominally) and of $Ti_5Si_3O_Y$ (Y = 0, 0.15, 0.25, 0.35, and 0.5; nominally) were determined from neutron diffraction. Scans were run from 10° to 110° with a source wavelength of 1.765 Å for samples with interstitial carbon and of 1.486 Å for samples with interstitial oxygen. Wavelength was selected by a curved monochromator, and a position-sensitive detector recorded intensities. Diffraction spectra were analyzed using the same Rietveld software as mentioned above. The wR_p was less than 0.06 for all refined neutron spectra, and the standard error for atomic position measurements was less than 0.0003 Å. The titanium positions, x_{Ti}, refined from neutron diffraction spectra were within 0.5% of those refined from x-ray spectra. However, unlike the x_{Ti} positions, the correlation between the x_{Si} positions obtained from neutron and XRD spectra was poor. This difference may be attributed to a smaller x-ray cross section for silicon atoms relative to titanium atoms. For this reason, the x_{Si} positions obtained from XRD spectra were not used in atomic separation calculations.

Oxygen and nitrogen content were measured on a TC-436 analyzer (Leco, St. Joseph, MO); carbon content was measured on a Model EMIA-520 analyzer (Horiba, Tokyo, Japan). The accuracy of these instruments, based on calibration standards, are reported to be ±2% relative for carbon, ±4% for oxygen, and ±10% for nitrogen. Samples were submillimeter-size granules weighing 0.2 to 0.5 g, total. The total carbon, nitrogen, and oxygen impurities for all samples, as measured by these techniques, were less than 0.02 formula units. However, samples with oxygen or nitrogen intentionally added showed less nitrogen and oxygen than the nominal starting composition (up to 20 wt% less for samples with a nominal interstitial content greater than 0.5 formula units). This validates the statement that some of the measured weight loss during arc melting was due to the volatilization of oxygen or nitrogen. In contrast, the measured carbon content of samples with carbon intentionally added was within 6 wt% of the nominal composition.

The carbon and oxygen content, as measured by chemical analysis, were within 5 wt% of the site occupancy refinements obtained from the neutron diffraction spectra, a difference that is similar to the expected accuracy of both measurement techniques. The fact that chemical analysis and neutron diffraction yielded identical results (within measurement accuracy) provides direct evidence that the vast majority of the carbon and oxygen (and nitrogen) in the arc-melted ingots are located in the interstices at (0, 0, 0) in $Ti_5Si_3Z_X$ as was anticipated.

III. RESULTS AND DISCUSSION

A. X-ray spectra

Figure 2 gives the experimental and calculated x-ray spectra of $Ti_5Si_3O_{0.019}$ and $Ti_5Si_3C_{0.47}$. Most x-ray spectra confirmed that samples were single phase and well crystallized. Samples that were not single phase included $Ti_5Si_{3.12}$, $Ti_5Si_3C_{1.0}$, and $Ti_5Si_3O_{1.0}$, which were intentionally synthesized in two-phase regions. Note the difference in (100) peak intensity relative to the (110) peak intensity for the two spectra as illustrated in Fig. 2. The ratio of the (100) to (110) integrated peak intensity as a function of interstitial content is plotted in Fig. 3. Integrated intensities were determined by fitting both diffraction lines to a Pearson VII profile. As a first-order approximation, the interstitial content of Ti_5Si_3 can be estimated by using the integrated intensity ratio of the (100) and (110) peaks and comparing to Fig. 3. However, longer counting times are required to accurately estimate interstitial content below approximately 0.1 and above 0.5 formula units. At these levels of interstitial content, one of the two peaks was generally too small to accurately estimate the intensity.

Plotted in Fig. 3 are also the calculated integrated intensity trends for Ti_5Si_3 with carbon or oxygen incorporations. These trends were calculated by

$$I^{100}/I^{110} = [S \cdot L_p{}^{100} \cdot M^{100} \cdot |F^{100}|^2]/[L_p{}^{110} \cdot |F^{110}|^2] \quad . \qquad (2)$$

L_p is the Lorentz-polarization term, M is the line multiplicity (equal to 6 for both lines), $|F|^2$ is the square of the structure factor, and S is a scaling factor equal to approximately 0.5. The need for a scaling factor is most likely due to neglecting an absorption coefficient, or less likely, due to preferred orientation. Thus, this scaling factor will be different for different types of diffractometers. As such, one would need one sample of known composition to adjust the trend in Fig. 3 for a different diffractometer. Although the explicit expressions for the calculated trends are quite unwieldy, by ignoring the anomalous dispersion correction to the scattering factors, good approximation is obtained:

$$\frac{I^{100}}{I^{110}} = \frac{S[A_Z^{100}X + 2A_{Ti}^{100}\cos(2\pi x_{Ti}) + A_{Si}^{100}(2\cos(2\pi x_{Si}) + 1)]^2}{[A_Z^{110}X + A_{Ti}^{110}(\cos(2\pi x_{Ti}) + \cos(4\pi x_{Ti}) + 2 + A_{Si}^{110}(\cos(2\pi x_{Si}) + \cos(4\pi x_{Si}))]^2} \quad , \tag{3}$$

$$A_{atom}^{hkl} = 2f_{atom}^{hkl} \cdot T_{atom}^{hkl} \cdot (L_p^{hkl})^{1/2} \quad . \tag{4}$$

Regarding Eqs. (3) and (4), X is the interstitial content, f_{atom}^{hkl} is the atomic scattering factor, and T_{atom}^{hkl} is the thermal parameter for a particular atom and for a given diffraction line. The scattering factors, thermal parameters, and Lorentz-polarization term are actually functions of X because incorporation of interstitial atoms changes the lattice and hence, slightly shifts a given diffraction line. However, for the refinement calculations, this X-dependence is quite negligible. However, the atomic positions x_{Ti} and x_{Si}, which are also (linear) functions of X (see Fig. 5), must be treated as such to more accurately model the integrated intensity ratio.

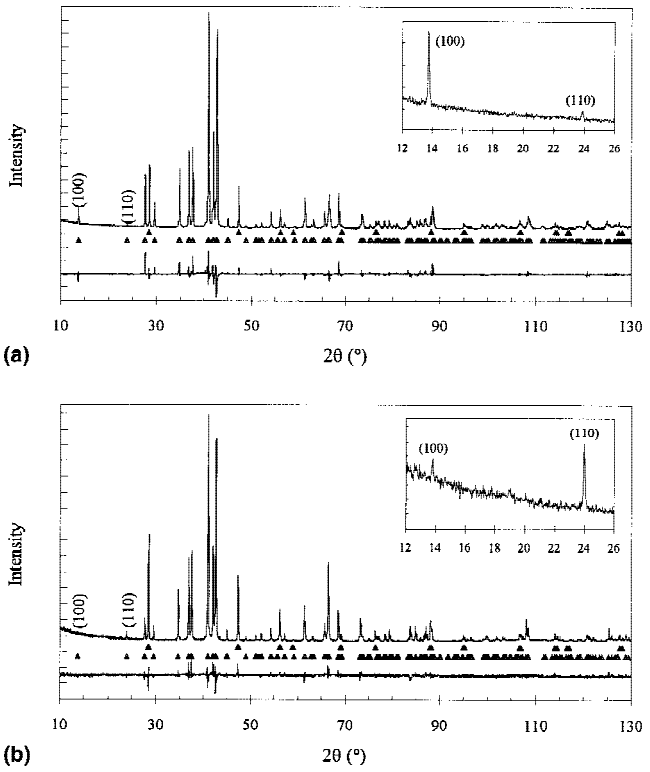

FIG. 2. XRD spectra of (a) $Ti_5Si_3O_{0.019}$ and (b) $Ti_5Si_3C_{0.47}$. From top to bottom of each plot are diffraction spectrum, silicon peak markers, Ti_5Si_3 peak markers, and difference plot. The difference plot is the difference between the observed spectra and the calculated spectra using Rietveld refinement.

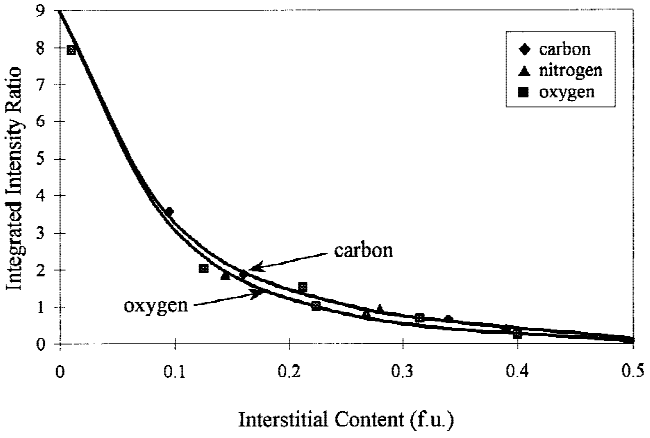

FIG. 3. Measured integrated intensity ratio of (100) peak divided by (110) peak. Solid curves represent theoretical integrated intensity ratios based on carbon or oxygen additions.

B. Lattice parameters and atomic positions

Figure 4 gives the changes in lattice parameters of Ti_5Si_3 as a function of interstitial content. The horizontal error bars represent the accuracy of measuring the carbon, nitrogen, and oxygen content (see Sec. II). The vertical error bars represent 3σ, where σ is the average standard deviation of three replicate measurements of five different compositions. Along each ordinate is a bar that marks the range of lattice values reported in the literature for supposedly pure Ti_5Si_3. Based on this figure, the scatter in reported lattice parameters can be explained by combinations of interstitial carbon, nitrogen, and oxygen, as well as excess silicon. The large expansion of the lattice due to the addition of excess silicon suggests that excess silicon also occupies the interstitial position. Also, note that the trends in lattice parameters as a function of carbon, oxygen, and nitrogen all converge to a similar value when extrapolated to zero interstitial content. The lattice parameters for pure Ti_5Si_3, as listed in Table I, were determined by extrapolating the oxygen trends to the zero interstitial level. Similarly, x_{Ti} and x_{Si} for pure Ti_5Si_3 were calculated by extrapolating the atomic position data shown in Fig. 5. These values are in good agreement with those found by Kajitani *et al.*[1] Additionally, most trends show a relative extremum near the 0.5 interstitial level, which corresponds to the point at which the interstices become more than half

filled. The reason for the extrema may be due to close Z–Z separations, which will be discussed in Sec. III. C.

Although not shown, excess titanium actually causes a relatively negligible contraction of the lattice. This would indicate that, unlike excess silicon, excess titanium is not incorporated into the Z site at (0, 0, 0). However, this result should be regarded with caution because samples with excess silicon and titanium almost certainly require thermal annealing after arc melting to achieve an equilibrium state. The reason is that unlike the other samples which solidified congruently, samples with excess silicon and titanium were in a two-phase region during solidification; and as such, these samples most likely had a significant chemical heterogeneity. Evidence for this was manifested as broader diffraction lines than the single-phase compositions.

Also plotted in Fig. 4 are the powder XRD data of Thom *et al.*[14] The much larger vertical error bars from Thom *et al.*[14] are due to samples that are more heterogeneous and/or a lack of an internal standard during XRD. Regardless of these imprecisions, the trends in lattice parameters between studies are similar.

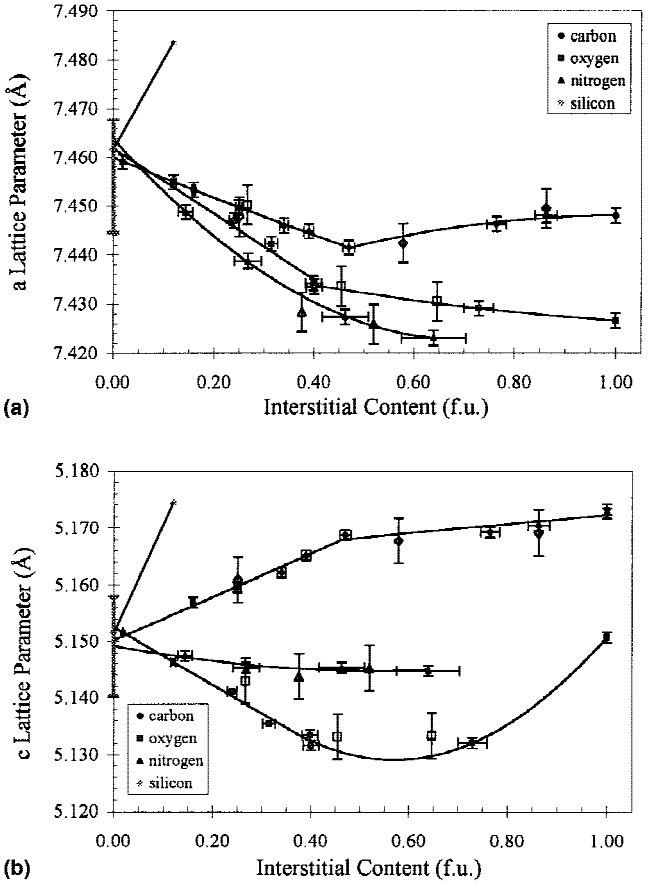

FIG. 4. Changes in the (a) *a*-lattice parameter or (b) *c*-lattice parameter as a function of formula units (f.u.) of interstitial atoms. The open symbols represent data taken from Thom *et al.*[14] The bars along the ordinate represent literature values for reportedly pure Ti_5Si_3. Values extrapolated back to zero were attributed to truly pure Ti_5Si_3.

C. Atomic separations

Nearest-neighbor separations in Ti_5Si_3 calculated from the extrapolated structural parameters are listed in Table II and are illustrated in Fig. 1. Based on first-principle calculations, bonding in Ti_5Si_3 primarily consists of *d*(Ti)–*p*(Si) covalent bonding below the Fermi level and *d*(Ti)–*d*(Ti) interaction at and around the Fermi level.[15] The crystal structure and atomic separations suggest that most of the *d*(Ti)–*p*(Si) bonding falls in the B and C planes and most of the *d*(Ti)–*d*(Ti) interaction parallel to the *c* axis. For example, three of the five nearest silicon atoms to Ti^{6g} (Ti^{6g}–Si II and Ti^{6g}–Si III) lie in the (001) plane; the others (Ti^{6g}–Si I) lie approximately 68° above/below this plane but are 5% to 7% farther away. In addition, the six silicon atoms surrounding Ti^{4d} lie only 29° above/below the (001) plane and thus have a significantly larger bonding component in the (001) plane. In the case of *d*(Ti)–*d*(Ti) interaction, all of the Ti nearest neighbors to Ti^{4d} lie along the *c* axis, and

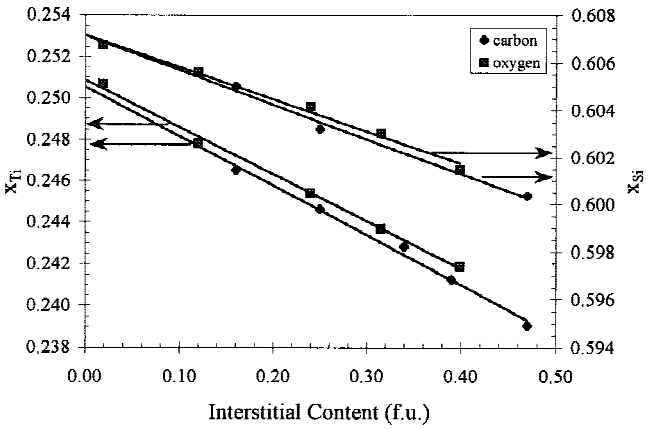

FIG. 5. Atomic positions, x_{Ti} and x_{Si}, as a function of formula units (f.u.) of carbon or oxygen. Values extrapolated back to zero were attributed to pure Ti_5Si_3.

TABLE I. Extrapolated lattice data for Ti_5Si_3.

	a, Å	*c*, Å	x_{Ti}	x_{Si}
This Study[a]	7.460 ± 0.002	5.152 ± 0.002	0.2509 ± 0.0005	0.6072 ± 0.0005
Kajitani *et al.*[1]	7.4610 (3)	5.1508 (1)	0.2473 (9)	0.6063 (9)

[a]Errors for this study represent 90% confidence intervals.

four of the six Ti nearest neighbors to Ti^{6g} lie 54° above/below the (001) plane. Also note that the Ti^{6g} atomic separations are over 23% longer than the Ti^{4d} separations; therefore, the Ti^{6g} atomic interactions are expected to be much weaker. This picture of weak metallic bonding in the ⟨001⟩ direction and strong covalent bonding in the ⟨100⟩ direction is corroborated by other experimental evidence: Both the electrical conductivity and thermal expansion are roughly twice as large along the ⟨001⟩ direction than along the ⟨100⟩ direction.[7]

The change in atomic separations as carbon or oxygen is added to Ti_5Si_3 is illustrated in Fig. 6. As seen in Fig. 6, the changes due to carbon and oxygen are in general very similar. The most dramatic effects are the decrease of the Ti^{6g}–Ti^{6g} and Ti^{6g}–Z separations and increase of the Ti^{6g}–Si separations as interstitial content increases. These effects are a direct result of increased bonding between the Ti^{6g} and interstitial Z atoms and a possible reduction in bonding between the Ti^{6g} and Si atoms. Based on these bonding changes, one might expect a reduction of covalent bonding in the ⟨100⟩ direction and an increase of covalent/ionic bonding in the ⟨001⟩ direction. This is in full agreement with Thom *et al.*[5] who showed an increase in the thermal expansion along the ⟨100⟩ direction and a decrease along the ⟨001⟩ direction as carbon is added to Ti_5Si_3.

Further insight into the bonding may be inferred by comparing atomic separations in $Ti_5Si_3Z_X$ to other compounds. One comparison, as mentioned by Ekman and Ozolins,[15] is that the Ti^{4d}–Ti^{4d} separation in $Ti_5Si_3Z_X$ is approximately 10% shorter than in titanium metal. This close separation is probably a result of significant electronic mixing with the six surrounding silicon atoms and a consequent reduction in orbital mixing between the two surrounding titanium atoms. In fact, the Ti^{4d}–Si separations in $Ti_5Si_3Z_X$ are only 1% to 2% longer than the shortest Ti–Si separation seen in $TiSi_2$—a compound with very strong Ti–Si covalent mixing. However, direct $d(Ti^{4d})$–$d(Ti^{4d})$ interaction must also exist according to densities of state calculations. Based on electron deformation maps, Ekman and Ozolins[15,16] suggested that the electronic mixing between Ti and Si atoms is best described by complex multicentered bonds and not by simple two-atom covalent bonds.

Another useful comparison is made between $Ti_5Si_3Z_X$ and TiZ for Z = carbon or oxygen. Both TiC and TiO form in the NaCl crystal structure; thus, the carbon and oxygen atoms are surrounded by six titanium atoms similar to the octahedral coordination found in $Ti_5Si_3Z_X$. However, the Ti–O separation in $Ti_5Si_3O_X$ is 6 to 8% longer than in TiO, and the Ti–C separation in $Ti_5Si_3C_X$ is 2% to 4% longer than in TiC. Additionally, whereas the coordinate octahedra in $Ti_5Si_3Z_X$ are face shared, the octahedra in TiZ are edge shared. The face-shared octahedra in $Ti_5Si_3Z_X$ result in significantly closer Z–Z separations than those in TiZ. Whereas Ti–Z bonding leads to lattice contraction below 0.5 formula units of Z, the short Z–Z separations may be the cause of subsequent lattice expansion as more than 0.5 formula units of Z atoms are added.

IV. CONCLUSIONS

Much of the research on the properties of Ti_5Si_3 is marred by the presence of uncontrolled impurities of carbon, nitrogen, and oxygen. This is readily seen by comparison of reported lattice parameters to the measured

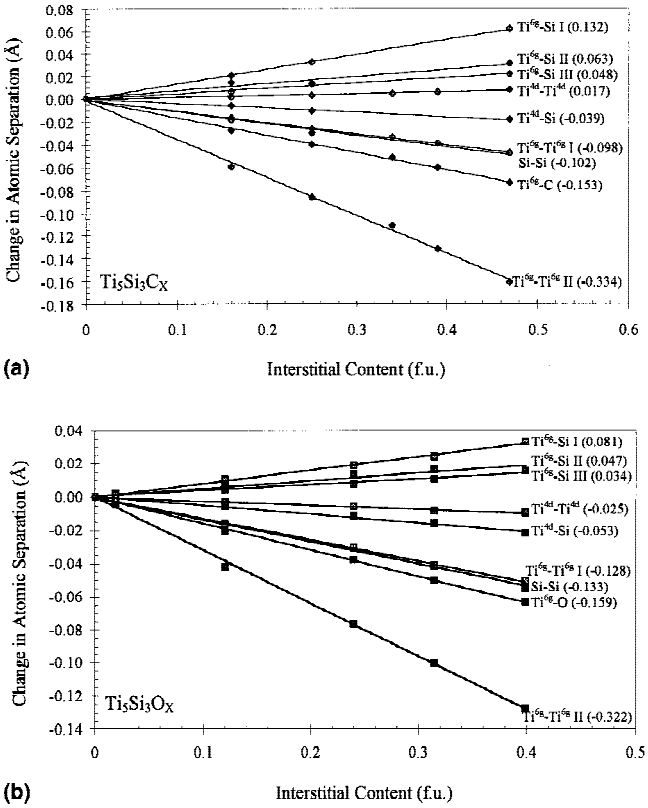

FIG. 6. Difference in atomic separations relative to atomic separations in Ti_5Si_3 for (a) $Ti_5Si_3C_X$ or (b) $Ti_5Si_3O_X$. The zero level (Ti_5Si_3) is based on extrapolated values listed in Table I. The values in parentheses are slopes of least-squares fitted lines in units of angstroms/formula units.

TABLE II. Calculated atomic separations for Ti_5Si_3 in angstroms.

Ti^{6g}–Si I	Ti^{6g}–Si II	Ti^{6g}–Si III	Ti^{6g}–Ti^{6g} I	Ti^{6g}–Ti^{6g} II	Si–Si	Ti^{4d}–Si	Ti^{6g}–Z	Ti^{4d}–Ti^{4d}
2.785	2.658	2.570	3.184	3.242	3.032	2.634	2.272	2.576

trends in lattice parameters as carbon, nitrogen, or oxygen is intentionally added to Ti_5Si_3. The amount of interstitial contamination can be quickly estimated by measuring the integrated intensity ratio of the (100) and (110) diffraction peaks. Additionally, the highly anisotropic thermal expansion of Ti_5Si_3 is a direct result of strong covalent bonding in the (001) planes and metallic bonding along the ⟨001⟩ direction. However, additions of interstitial atoms change the bonding such as to reduce this anisotropy. These changes in bonding were seen in the effect interstitial atoms have on atomic separations. The most significant changes include the reduction of Ti^{6g}–Ti^{6g} and Ti^{6g}–Z distances and the expansion of Ti^{6g}–Si distances. This suggests a relative increase of covalent/ionic bonding along the ⟨001⟩ direction and a relative reduction of covalent bonding in the (001) planes.

ACKNOWLEDGMENTS

Assistance provided by Dr. Andrew J. Thom during the course of this investigation is greatly appreciated. Ames Laboratory is operated for the United States Department of Energy by Iowa State University under Contract No. W-7405-ENG-82. The work at MURR was supported by the United States Department of Energy Grant No. DE-FE02-90ER45427.

REFERENCES

1. T. Kajitani, T. Kawase, K. Yamada, and M. Hirabayashi Trans. Jpn. Inst. Metals **27,** 639 (1986).
2. D.G. Archer, D. Filor, E. Oakley, and E. Cotts, J. Chem. Eng. Data **41,** 571 (1996).
3. R. Mitra, Metall. Mater. Trans. A **29,** 1629 (1998).
4. R. Rosenkranz, G. Frommeyer, and W. Smarsly, Mater. Sci. Eng. A **152,** 288 (1992).
5. A.J. Thom, M. Akinc, O.B. Cavin, and C.R. Hubbard, J. Mater. Sci. Lett. **13,** 1657 (1994).
6. L. Zhang and J. Wu, Scripta Mater. **38,** 307 (1998).
7. T. Nakashima and Y. Umakoshi, Philos. Mag. Lett. **66,** 317 (1992).
8. Y. Ikarashi, K. Ishizaki, T. Nagai, Y. Hashizuka, and Y. Kondo, Intermet. **4,** 141 (1996).
9. I. Barin, *Thermochemical Data of Pure Substances*, 2nd ed., (VCH, Weinhiem, Germany, 1993).
10. H.J. Seifert, H.L. Lukas, and G. Petzow, Z. Metallkd. **87,** 2 (1996).
11. R. Radhakrishnan, J.J. Williams, M. Kramer, and M. Akinc, Ceram. Eng. Sci. Proc. **19,** 381 (1998).
12. A.J. Thom and M. Akinc, Ceram. Eng. Sci. Proc. **18,** 57 (1997).
13. J. Quakernaat and J.W. Visser, High Temp. High Press. **6,** 515 (1974).
14. A.J. Thom, V.G. Young, and M. Akinc, J. Alloys Compds. **296,** 59 (2000).
15. M. Ekman and V. Ozolins, *Properties of Complex Inorganic Solids*, edited by A. Gonis (Plenum Press, New York, 1997), p. 191.
16. M. Ekman and V. Ozolins, Phys. Rev. B: Solid State. **57,** 4419 (1998)